Available online at www.sciencedirect.com

ScienceDirect

J. Chem. Thermodynamics 40 (2008) 25–31

JCT

www.elsevier.com/locate/jct

Phase behavior of {carbon dioxide + [bmim][Ac]} mixtures

Mark B. Shiflett [a,*], Daniel J. Kasprzak [a], Christopher P. Junk [a], A. Yokozeki [b]

[a] *DuPont Central Research and Development, Experimental Station, Wilmington, DE 19880, USA*
[b] *DuPont Fluoroproducts Laboratory, Chestnut Run Plaza 711, Wilmington, DE 19880, USA*

Received 3 February 2007; received in revised form 23 May 2007; accepted 4 June 2007
Available online 12 June 2007

Abstract

Carbon dioxide solubility {(vapor + liquid) equilibria: VLE} in ionic liquid, 1-butyl-3-methylimidazolium acetate ([bmim][Ac]), has been measured with a gravimetric microbalance at four isotherms about (283, 298, 323, and 348) K up to about 2 MPa. (Vapor + liquid + liquid) equilibria (VLLE: or liquid–liquid separations) have also been investigated with a volumetric method used in our previous works, since the present analysis of the VLE data using our equation-of-state model has predicted the VLLE at CO_2-rich side solutions. The prediction for the VLLE has been confirmed experimentally. CO_2 solubilities at the ionic liquid-rich side show extremely unusual behaviors; CO_2 dissolves in the ionic liquid to a great degree, but there is hardly any vapor pressure above these mixtures up to about 20 mol% of CO_2. It indicates that CO_2 may have formed a non-volatile or very low vapor pressure molecular complex with the ionic liquid. The thermodynamic excess properties (enthalpy, entropy, and Gibbs free energy) of the present system do support such a complex formation. We have conducted several other experiments to investigate the complex formation (or chemical reactions), and conclude that a minor chemical reaction occurs but the complex formation is reversible without much degradation of the ionic liquid.

Keywords: Carbon dioxide; Solubility; Ionic liquid; Equation of state; Phase equilibria; Liquid–liquid separation; Molecular complex formation

1. Introduction

Various applications of a new class of compounds, room-temperature ionic liquids (RTILs), have been widely proposed in the last several years. RTILs are molten salts at room temperature without practically any vapor pressure and thus regarded as “green solvents”, due to the lack of volatile organic compounds (VOCs).

Among many possible RTIL applications, a promising application may be the capture (or sequestration) of sour gases like CO_2, H_2S, and SO_2 in refinery, coal combustion, and synthesis of gas streams, using the unique absorption characteristics of RTILs. Researchers at the University of Notre Dame, E.J. Maginn, J.F. Brennecke and their co-workers, have initiated such studies a few years ago, and are making steady progress in this area, as described in their Technical Reports to DOE (Department of Energy, USA) [1]. One of their RTILs for the CO_2 solubility studies is 1-butyl-3-methylimidazolium acetate, [bmim][Ac], which shows very high solubility of CO_2. Their results imply possible chemical reactions [1], although their experimental solubility data at only one temperature have been quite limited. In this respect, Chinn *et al.* have proposed the {CO_2 + [bmim][Ac] + water} system as the CO_2 absorbent (or sequestration) in their US patent [2].

The purpose of the present study is to re-examine in detail their findings of the very high solubility of CO_2 in [bmim][Ac] and to shed some light on this interesting binary system. To do so, we measured more detailed solubility data {(vapor + liquid) equilibria: VLE} than those in the literature. Then, we made a thermodynamic model for this system using an equation of state, which has predicted a very rare phase behavior including liquid–liquid separations {(vapor + liquid + liquid) equilibria: VLLE}. VLLE are confirmed experimentally for the first time in this system. Furthermore, in order to understand possible

---

[*] Corresponding author. Tel.: +1 302 695 2572; fax: +1 302 695 4414.
E-mail address: mark.b.shiflett@usa.dupont.com (M.B. Shiflett).

0021-9614/$ - see front matter © 2007 Elsevier Ltd. All rights reserved.
doi:10.1016/j.jct.2007.06.003

chemical reactions or complex formation in the present system, we have conducted several other experiments: making CO_2 absorbed [bmim][Ac] solutions, and analyzing them by ^{1}H NMR, TGA-IR, FT-IR and ATR-IR for various sample conditions. Some reasonable models are discussed for the chemical and thermodynamic behaviors of this binary system.

2. Experimental

2.1. Materials

Carbon dioxide (purity >0.9999 mass fraction, CAS no. 124-38-9) was purchased from MG Industries (Philadelphia, PA). The [bmim][Ac] (assay ⩾0.95 mass fraction, $C_{10}H_{18}N_2O_2$, CAS no. 284049-75-8, Lot and Filling code S25803 444041302) was obtained from Fluka (Buchs, Switzerland). The as-received mass fraction of water was measured by Karl–Fischer titration (Aqua-Star C3000, solutions AquaStar Coulomat C and A) and the undried sample contained 4699 ppm H_2O. The [bmim][Ac] was dried and degassed by first filling a borosilicate glass tube with about 10 g of ionic liquid and pulling a coarse vacuum with a diaphragm pump (Pfeiffer, model MVP055-3, Nashua, NH) for about 3 h. Next, the [bmim][Ac] was completely evacuated using a turbopump (Pfeiffer, model TSH-071) to a pressure of about $4 \cdot 10^{-7}$ kPa while simultaneously heating and stirring the ionic liquid at a temperature of about 348 K for 5 days. The final mass fraction of water was agained measured by Karl–Fischer titration and the dried sample contained 703 ppm H_2O.

Detailed descriptions of experimental equipment and procedures for the VLE and VLLE are given in our previous reports [3–6]; therefore, only the basic experimental techniques and measurement uncertainties are presented here.

2.2. VLE apparatus

The gas solubility (VLE) measurements were made using a gravimetric microbalance [3] (Hiden Isochema Ltd., IGA 003, Warrington, United Kingdom). A molecular sieve trap was installed to remove trace amounts of water from the CO_2. Initially, about 66.7 mg of [bmim][Ac] was loaded into the sample container and heated to 348.15 K under a vacuum of about 10^{-9} MPa for 10 h to remove any trace amounts of water or other volatile impurities. The final mass after drying was 61.5 mg with a resulting mass loss of 7.8%. The as received water content of 4699 ppm accounts for only a portion of the mass loss. We believe the remaining mass loss is due to both volatile impurities and the small but non-negligible [bmim][Ac] vapor pressure.

The IGA003 apparatus can operate in both dynamic (continuous gas flow) and static (intermittent gas flow) modes. Absorption and desorption measurements were performed in static mode in this study. The sample temperature was measured with a type K thermocouple with an accuracy of ±0.1 K. The thermocouple was calibrated using a standard platinum resistance thermometer (SPRT model 5699, Hart Scientific, American Fork, UT, range 73 K to 933 K) and readout (Blackstack model 1560 with SPRT module 2560). The Blackstack instrument and SPRT are a certified secondary temperature standard with a NIST traceable accuracy to ±0.005 K. Four isotherms of about (283, 298, 323, and 348) K were measured beginning with 298 K. Pressures from (10^{-2} to 2.0) MPa were measured using a piezo-resistive strain gauge (Druck, model PDCR4010) with an accuracy of ± 0.8 kPa. The Druck pressure transducer was calibrated against a Paroscientific model 760-6K (Redmond, WA) pressure transducer (range 0 MPa to 41.5 MPa, serial no. 62724). This instrument is also a NIST certified secondary pressure standard with a traceable accuracy of 0.008% of full scale. The upper pressure limit of the microbalance reactor was 2.0 MPa, and several isobars up to 2.0 MPa {(0.01, 0.05, 0.1, 0.4, 0.7, 1.0, 1.3, 1.5, and 2.0) MPa} were measured in the present study. In our previous reports [3–6], to ensure sufficient time for VLE, each T, P condition was maintained for a minimum of 3 h with a maximum time of 8 h. In this work, we found that 8 h was not sufficient to reach equilibrium particularly at (283 and 298) K. Therefore, a maximum of 10 h was set for isotherms measured at (298, 323, and 348) K and a maximum of 20 h for the 283 K isotherm. Absorption and desorption isotherms were measured at (283 and 298) K and the average molar composition for the absorption and desorption T, P condition is shown in table 1. The CO_2 mass uptake *versus* time for absorption and desorption experiments between (0 and 1) bar at 298 K indicates a reversible chemical complex may have formed, since additional time was required to desorb the CO_2 and the need to heat the sample to obtain the same initial ionic liquid mass.

The instrumental uncertainties in T and P are within ±0.1 K and ±0.8 kPa, respectively. These uncertainties do not cause any significant effects in the gas solubility measurement. The total uncertainties in the solubility data due to both random and systematic errors have been estimated to be less than 0.006 mole fraction at given T and P except for low temperature cases (283 K and 298 K). Uncertainties due to hysteresis between absorption and desorption isotherms at (283 and 298) K are significantly larger. Another large source of uncertainty in the present solubility experiments is due to the buoyancy correction in the data analysis. Analysis of the buoyancy effects requires an accurate measurement of the [bmim][Ac] liquid density and CO_2 gas density [7]. Liquid density data for [bmim][Ac] by BASF ($1.055\ g \cdot cm^{-3}$ at 298.15 K and $1.0192\ g \cdot cm^{-3}$ at 353.15 K) [8] were used in our analysis, and they were correlated as $d\ (g \cdot cm^{-3}) = 1.24907$ to $6.50905 \cdot 10^{-4}\ T/K$. The [bmim][Ac] liquid density was also measured using a 1.0 ml pycnometer ($1.053 \pm 0.001\ g \cdot cm^{-3}$ at 298.15 K) and found to be in good agreement with the BASF measurement. In the case of CO_2 absorbing in

TABLE 1
Experimental solubility (P, T, x) data for $\{CO_2\ (1) + [bmim][Ac]\ (2)\}$

T/K	P/MPa	$100x_1$
283.1	0.0102	19.2 ± 7.3^a
283.1	0.0502	27.3 ± 2.1^a
283.1	0.1002	30.7 ± 0.4^a
283.1	0.3997	35.7 ± 0.1^a
283.1	0.6994	39.3 ± 0.0^a
298.1	0.0101	18.8 ± 2.6^a
298.1	0.0502	25.2 ± 0.2^a
298.1	0.1003	27.4 ± 0.2^a
298.1	0.3999	32.4 ± 0.2^a
298.1	0.7002	35.5 ± 0.2^a
298.1	0.9996	38.1 ± 0.2^a
298.2	1.3001	40.5 ± 0.1^a
298.1	1.5001	42.0 ± 0.1^a
298.1	1.9994	45.5 ± 0.0^a
323.1	0.0104	10.8
323.1	0.0504	17.6
323.1	0.1004	20.4
323.1	0.3995	26.3
323.2	0.7003	29.2
323.1	1.0001	31.5
323.1	1.3002	33.4
323.1	1.4995	34.6
323.2	1.9993	37.3
348.1	0.0104	6.3
348.1	0.0505	12.9
348.1	0.1000	16.1
348.1	0.4002	22.6
348.1	0.6994	25.3
348.1	1.0003	27.2
348.1	1.2994	28.7
348.1	1.4997	29.4
348.2	1.9993	31.6

[a] Average of absorption and desorption isotherm.

[bmim][Ac] the change in molar liquid volume at the measured T, P conditions is from 0% to −36%, with a measurable affect on the final solubility measurements of 0% to +2% (in mol%). A detailed description of the buoyancy correction and change in molar liquid volume calculation are provided in our previous report [3]. The corrected solubility (P, T, x) data are shown in table 1.

2.3. VLLE apparatus

High-pressure sample containers were filled with dried [bmim][Ac] following the procedures outlined in our recent publications [4,5]. VLLE experiments have been made with these samples at constant temperatures of about (281, 289, and 292) K using the volumetric method [4,5]. The VLLE determined by this method required only mass-and-volume measurements without any analytical method for molar composition or volume analysis. Detail error analyses are also given in references [4,5]. The bath temperature was calibrated with the NIST traceable SPRT mentioned previously and the uncertainty in temperature was ± 0.2 K. Special attention must be given to ensure no leaks occur from the sample containers after being filled with the high-pressure CO_2. Weights of sample containers were checked several times before starting and after completing the VLLE experiments to ensure that no CO_2 had escaped from the sample container. It is also important to mention that the vapor phase density which contains CO_2 with a negligible contribution of [bmim][Ac] must be properly accounted for in the mass balance equations described in references [4,5]. Observed liquid phase compositions and molar volumes are shown in table 2.

2.4. CO_2 and [bmim][Ac] flow apparatus

An experimental apparatus was setup to continuously bubble CO_2 gas through a sample of [bmim][Ac] as shown in figure 1. The primary objective of this experiment was to generate material (CO_2 + [bmim][Ac]) for further analytical analysis. The CO_2 pressure was adjusted to 2.0 bar using a two-stage regulator. A drier trap (R&D Separations, model OT3-4, Rancho Cordova, CA) was installed to remove any oxygen or moisture from the CO_2 and the gas flow was regulated to $100 \pm 5\ cm^3 \cdot min^{-1}$ using a rotameter (Brooks Instruments, model 1355EYZZQFA1G, Hatfield, PA). A sample of 10.1816 g of undried [bmim][Ac] was added to a Pyrex® round bottom flask with a magnetic stir bar and placed on a stirring/heating plate (Corning, model PC-220, Acton, MA). The sample was agitated and the temperature was maintained at 293.2 ± 0.5 K. The temperature was measured using a type-K thermocouple, and a temperature controller (Eurotherm, model 2416, Leesburg, VA) adjusted the heat input. A stainless steel dip tube with a small orifice (0.5 mm) was inserted below the surface of the [bmim][Ac] above the stir bar for introducing the CO_2 gas. The top of the flask was sealed with a stopper and parafilm. A vent was installed to a bubbler filled with mineral oil to prevent air from reentering the flask. The CO_2 gas flowed through the [bmim][Ac] for 5 days. The sample was reweighed and the mass had increased 0.8403 g. Assuming the mass increase

TABLE 2
Experimental VLLE for $\{CO_2\ (1) + [bmim][Ac]\ (2)\}$

T/K	x'_1/mol%	x_1/mol%	$\overline{V}'^a/(cm^3 \cdot mol^{-1})$	$\overline{V}^a/(cm^3 \cdot mol^{-1})$	$\overline{V}^{ex'b}/(cm^3 \cdot mol^{-1})$	$\overline{V}^{ex b}/(cm^3 \cdot mol^{-1})$
281.1	72.3 ± 3.0	100.0 ± 0.4	69.7 ± 7.0	50.5 ± 4.0	-18.5 ± 7.0	-0.6 ± 4.0
288.7	70.5 ± 3.0	100.0 ± 0.4	73.0 ± 7.0	54.0 ± 4.0	-19.6 ± 7.0	0.1 ± 4.0
292.2	69.6 ± 3.0	100.0 ± 0.4	75.0 ± 7.0	54.9 ± 4.0	-20.0 ± 7.0	-0.6 ± 4.0

[a] Observed molar volume.
[b] Excess molar volume.

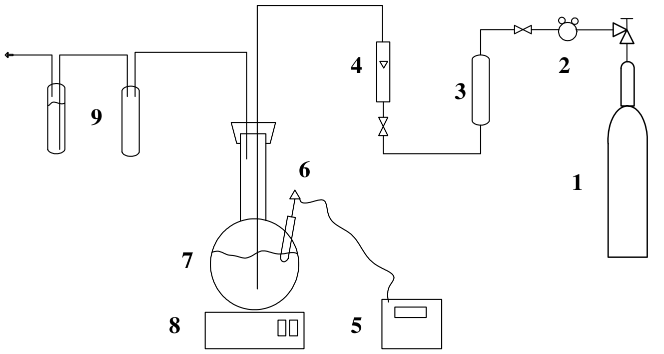

FIGURE 1. Schematic diagram of CO_2 bubbling apparatus. (1) High pressure CO_2 cylinder, (2) two-stage CO_2 regulator, (3) O_2/H_2O trap, (4) rotameter, (5) temperature readout, (6) thermocouple, (7) round bottom flask, (8) stirrer/heater, and (9) trap.

was only due to CO_2 absorption, results in 27.1 ± 1.0 mol% at 293.2 ± 0.5 K and 1.013 bar. This is in good agreement with the gravimetric microbalance results (28.4 ± 0.6 mol% at 293.2 K and 1.013 bar). In addition, a slight acetic acid odor was detected during sample weighing, indicating the occurrence of some chemical reaction. The sample was sealed and kept in a drybox for further analysis by ^{1}H NMR, thermogravimetric analysis/infrared (TGA-IR), Fourier transform infrared (FT-IR), and attenuated total reflectance infrared (ATR-IR).

2.5. ^{1}H NMR analysis

The molecular structure of [bmim][Ac] was verified by nuclear magnetic resonance (NMR). ^{1}H NMR spectra were recorded on a Bruker model DRX-500 spectrometer at 500.993 MHz using deuterated chloroform ($CDCl_3$) as the lock solvent. Three samples were analyzed, [bmim][Ac] (undried), [bmim][Ac] (dried), and a portion of the [bmim][Ac] with dissolved CO_2 from section 2.4. ^{1}H NMR spectra for each sample were similar. The integration of the ring hydrogens (labeled 4 and 5) to the ring hydrogen (labeled 2) shown in figure 2 for all three samples was the same within experimental uncertainty. This observation implies that any mechanism involving abstraction of the proton labeled 2 figure 2 must be a minor chemical reaction; further discussion about this fact is given later in section 2.4.

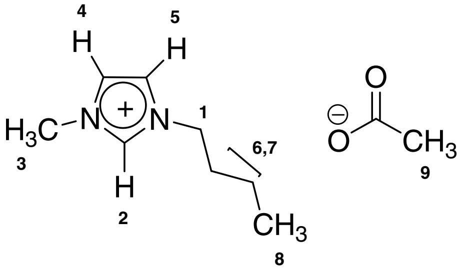

FIGURE 2. The chemical structure and numbering of the protons on the imidazolium cation ring and anion of [bmim][Ac].

2.6. TGA-IR analysis

Two ionic liquid samples 300 mg [bmim][Ac] (dried) and 400 mg [bmim][Ac] with dissolved CO_2 from section 2.4 were analyzed by thermogravimetric-infrared analysis (TGA-IR). The sample was positioned in the heating zone of the TGA (TA Instruments, model Q500 with EGA furnace, Newark, DE) inside a quartz tube. The tube was sealed and purged with a constant flow rate of dry nitrogen. The sample was heated from 303.15 K to 373.15 K at a ramp rate of $1.0\ K \cdot min^{-1}$ followed by a 2 min hold at 373.15 K. IR backgrounds were collected before the samples were added to the TGA. The evolved gases were swept through a 20 cm IR gas cell that was scanned continuously by the FT-IR spectrometer (Nicolet Nexus model 670, Thermo Electron Corporation, Waltham, MA). The IR gas cell was maintained at a temperature of about 623 K to avoid condensation of higher boiling components. The FT-IR spectrometer was operated at 4 cm^{-1} resolution with 28 scans co-added to yield a data point (spectrum) about every 30 s during the run.

The [bmim][Ac] had no detectable weight loss and only trace amounts of water and CO_2 (0.4 mg/g) were detected in the IR cell. The [bmim][Ac] with dissolved CO_2 had a measurable mass loss of 2.7%. Evolved gases included water and CO_2 (26.7 mg/g), but no acetic acid was detected (detection limit about 0.4 mg/g or 0.04%). Neglecting the H_2O contribution, this means that the CO_2 evolved here is about 24.4 mol%. This value is not inconsistent with the absorbed CO_2 measured (27.1 mol% in section 2.4) by considering the experimental uncertainties and that the temperature was only up to 373 K.

2.7. FT-IR analysis

Infrared spectra were collected on a Nicolet Magna 560 FT-IR spectrometer (Thermo Electron Corporation, Waltham, MA). The IR cell used for these studies consisted of a temperature-controlled, high-pressure cell mount (Wilmad, model 118-1P-1, Buena, NJ, USA) with 13 × 2 mm CaF_2 windows (International Crystal Laboratories, Garfield, NJ, USA), separated by a custom-made 12-μm Kaladex® polyethylene naphthalate spacer. For additional experimental details see reference [9].

IR spectra were collected at 298.15 K for both the [bmim][Ac] (undried) and the [bmim][Ac] with dissolved CO_2. In the (2000 to 4000) cm^{-1} region, a minor new peak appeared for the [bmim][Ac] with dissolved CO_2 at 2337 cm^{-1}. This is in the region where X=Y=Z type molecules absorb for out-of-phase stretch such as isocyanate (N=C=O). For reference, CO_2 in the gas phase absorbs near 2360 cm^{-1} [10] There was also a broad peak in both samples near 3350 cm^{-1} indicating the high water content mentioned previously. In the (900 to 2000) cm^{-1} region, new peaks showed up at (1668, 1509, and 1324) cm^{-1}. The new peaks suggest the presence of a carboxylate salt (COO^-). Other peaks were over-absorbed (>2.0) so

ATR-IR was used; therefore, all peaks would remain on scale.

2.8. ATR-IR analysis

The ATR unit was a Durasampl *IR* (Smiths Detection, Danbury, CT) with a diamond surface and a single bounce capability. The ATR unit was used in a Nicolet Magna 560Nexus FT-IR (Thermo Electron Corporation, Waltham, MA).

IR spectra were collected at about 296.15 K for both the [bmim][Ac] (undried) and the [bmim][Ac] with dissolved CO_2. In the (2000 to 4000) cm^{-1} region, the same new peak appeared for the [bmim][Ac] with dissolved CO_2 at 2337 cm^{-1}. In the (600 to 2000) cm^{-1} region, new peaks appeared at (1666, 1508, 1323, and 791) cm^{-1} as shown in figure 3. These peaks are consistent with those measured by FT-IR, except for the additional peak at 791 cm^{-1}. The 1173 cm^{-1} peak belongs with the [bmim] cation since it has appeared in many imidazolium based ionic liquids with different anions from past work [9] and can serve as a reference peak. The acetate carboxylate (C═O and C–O combined) peaks are at (1578 and 1379) cm^{-1}. An interesting parallel exists with the identification of peaks at (1666, 1323, and 791) cm^{-1} in [bmim][Ac] with dissolved CO_2 and with oxalate salts $(O_2C{-}CO_2)_2^{2-}$ which have peaks near (1620, 1320, and 770) cm^{-1} [11]. It may be possible that there are doubly charged CO_2 "dimers" interacting with the [bmim] cations. The overall intensity of the [bmim][Ac] spectrum containing dissolved CO_2 was lower than that of the pure [bmim][Ac], which indicates a decrease in the population of "normal" [bmim] and [Ac] species due to the presence of CO_2. Upon heating the sample to 323 K, these new peaks at (2337, 1666, 1508, 1323, and 791) cm^{-1} were significantly diminished, and at 352 K, the new peaks were virtually absent and the spectrum looked like pure [bmim][Ac]. These spectra combined with the TGA-IR results confirmed that the new peaks were due to CO_2 in solution and that the CO_2 reversibly evolved from the [bmim][Ac] at elevated temperature.

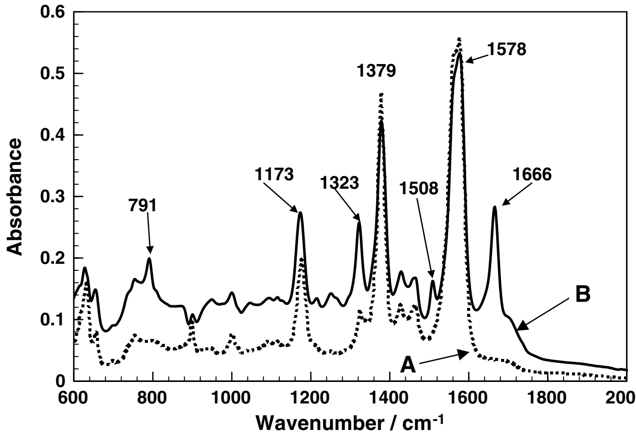

FIGURE 3. ATR-IR spectra of undried [bmim][Ac] (A, dashed line) and CO_2 + [bmim][Ac] (B, solid line).

3. Solubility data analysis and EOS predictions

Experimental solubility (VLE and VLLE) data are summarized in tables 1 and 2. In order to analyze these data, we employ a generic RK (Redlich–Kwong) type of cubic equations of state (EOS), which is written in the following form for a pure compound [12,13]:

$$P = \frac{RT}{V-b} - \frac{a(T)}{V(V+b)} \tag{1}$$

$$a(T) = 0.427480\frac{R^2T_c^2}{P_c}\alpha(T) \tag{2}$$

$$b = 0.08664\frac{RT_c}{P_c} \tag{3}$$

The temperature-dependent part of the *a* parameter in the EOS for pure compounds is modeled by the following empirical form [12,13]:

$$\alpha(T) = \sum_{k=0}^{\leqslant 3}\beta_k(1/T_r - T_r)^k, \quad (T_r \equiv T/T_C). \tag{4}$$

The coefficients, β_k, for each pure compound are determined so as to reproduce the vapor pressure. However, β_1 for non-volatile compounds such as ionic liquids is determined through the binary VLE data analysis using $\beta_0 = 1$ and $\beta_2 = \beta_3 = 0$, as described in our previous reports [12,13]. Pure component EOS parameters, including β_k, are listed in table 3.

Then, the *a* and *b* parameters for general *N*-component mixtures are modeled in terms of only binary interaction parameters [12,13].

$$a = \sum_{i,j=1}^{N} a_i a_j^{1/2} f_{ij}(T)(1-k_{ij})x_i x_j, \quad a_i = 0.427480\frac{R^2T_{ci}^2}{P_{ci}}\alpha_i(T), \tag{5}$$

$$f_{ij}(T) = 1 + \tau_{ij}/T, \quad \text{where} \quad \tau_{ij} = \tau_{ji} \quad \text{and} \quad \tau_{ii} = 0, \tag{6}$$

$$k_{ij} = \frac{l_{ij}l_{ji}(x_i + x_j)}{l_{ji}x_i + l_{ij}x_j}, \quad \text{where} \quad k_{ii} = 0, \tag{7}$$

$$b = \frac{1}{2}\sum_{i,j=1}^{N}(b_i + b_j)(1-k_{ij})(1-m_{ij})x_i x_j,$$

$$b_i = 0.08664\frac{RT_{ci}}{P_{ci}}, \tag{8}$$

where $m_{ij} = m_{ji}$, $m_{ii} = 0$. T_{ci} is critical temperature of the *i*-th species; P_{ci}, critical pressure of the *i*-th species; *R*, universal gas constant; and x_i is mole fraction of the *i*-th species.

In the above model, there is a maximum of four binary interaction parameters: l_{ij}, l_{ji}, m_{ij}, and τ_{ij} for each binary pair. These parameters have been determined by the non-linear least-squares analysis of binary VLE (P, T, x) data. The optimal binary interaction parameters thus obtained

TABLE 3
Pure component EOS parameters used in the present analysis[a]

Compound	Molar mass/$(g \cdot mol^{-1})$	T_c/K	P_c/kPa	β_0	β_1	β_2	β_3
CO_2	44.01	304.13	7385	1.0005	0.43866	−0.10498	0.06250
[bmim][Ac]	198.26	867.68	2942	1.0	1.34306	0	0

[a] The critical parameters for [bmim][Ac] were estimated with the method proposed by Vetere [17], using two liquid density data [8] and an assumed critical compressibility factor of 0.253.

TABLE 4
Binary interaction parameters[a] in equations (6) to (8)

System (1)/(2)	l_{12}	l_{21}	$m_{12} = m_{21}$	$\tau_{12} = \tau_{21}$/K
CO_2/[bmim][Ac]	0.11580	0.53511	−0.03976	79.594

[a] Determined by non-linear least-squares analyses using the VLE data of the present study. The standard deviation of the pressure fit is 0.04 MPa.

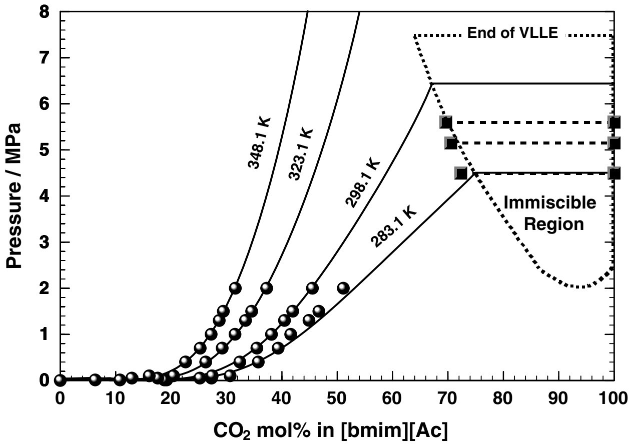

FIGURE 4. (P, T, x) phase diagram of the $\{CO_2 + [bmim][Ac]\}$ system. Solid and dotted lines: calculated by the present EOS model. Solid circles: the present experimental VLE data. Solid squares and broken lines: the present experimental VLLE data and the LLE tie lines.

are shown in table 4. The fugacity coefficient, which is needed for the phase equilibrium calculation, and other derived thermodynamic functions relevant to the present study are given in explicit forms for the present EOS in reference [12,14].

EOS model calculations for the four isothermal VLE are compared with the observed data in figure 4; the standard deviation of the pressure fit was 0.04 MPa. The present EOS has predicted the VLLE (or liquid–liquid separation) in the CO_2-rich side solution, as shown in figure 4 with the dotted line. This VLLE behavior has been well confirmed by the present VLLE experiment (table 2); these experimental data are also compared in figure 4.

4. Discussion

The binary system of $\{CO_2 + [bmim][Ac]\}$ has shown highly unusual phase behaviors. At low CO_2 concentrations (less than *ca.* 20 mol%), the binary mixtures have hardly any vapor pressures, reflecting a strong attractive (or complex formation) interaction between CO_2 and [bmim][Ac], while at high CO_2 concentrations (above *ca.* 70 mol%), the binary solutions show liquid–liquid separations (or immiscible VLLE). Such a highly asymmetric phase behavior with respect to concentrations is extremely rare [15], and one of the few known examples is a binary system of HCl and water [15,16].

The present EOS model has successfully correlated the unusual VLE (solubility) data, and even predicted the VLLE behavior at high CO_2 concentrations. VLLE experiments have proven such a prediction for the first time for the present binary system. The numerical agreement between the predicted and experimental values as shown in figure 4 is not as good as our previous work [6]. However, it should be noted that the present binary system may not be strictly a binary system but possibly a ternary system of $\{CO_2 + [bmim][Ac] + water\}$, since the water content in [bmim][Ac] was significantly high even after being “dried.” In addition, the system may contain small amounts of reaction products as discussed below. By considering these effects, the agreement shown in figure 4 may be said to be surprisingly good, assuming the system as being pseudo-binary in the present EOS and VLLE analyses. The VLLE experiments have also provided the excess molar volume of this binary system, and show large negative values in the ionic-liquid rich side solutions, as shown in table 2. The large negative excess molar volumes found in the $\{CO_2 + [bmim][Ac]\}$ system are very similar to results of our previous work on CO_2 + [hmim][Tf_2N] [6] and hydrofluorocarbons + [bmim][PF_6] [4,5].

As mentioned above, the present system possesses strong attractive intermolecular interactions. One of the best ways to observe such behaviors is to look at the thermodynamic excess functions. Figure 5 shows the excess functions (excess Gibbs free energy, enthalpy, and entropy) at 298 K, calculated based on the present EOS model. All the excess functions are large negative except for high CO_2 concentrations, thus clearly indicating the possibility of intermolecular complex formations or chemical reactions. In this respect, Maginn [1] proposed a chemical reaction for this binary system as shown in figure 6. The reaction product is acetic acid and a stable adduct of imidazolium carboxylate. This reaction very likely happens to some extent, since we have in fact smelled acetic acid mentioned in section 2.4. However, the amount of such a chemical reaction must be minor for two reasons. First, if the proton labeled 2 (figure 2) is being removed (as shown in figure 6) the ^1H NMR integration ratio (ring hydrogen labeled 4 and 5 to ring hydrogen labeled 2) should increase

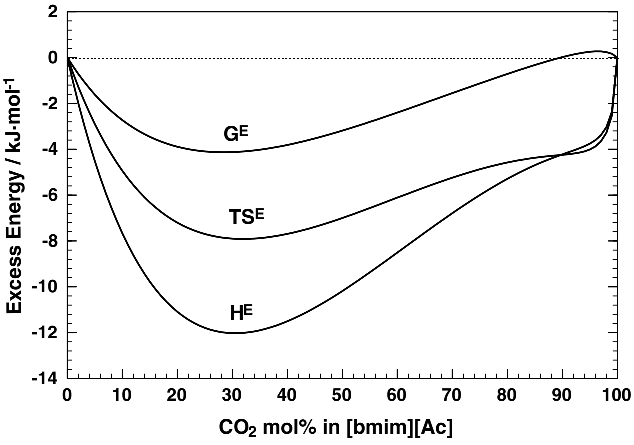

FIGURE 5. Excess properties (enthalpy, entropy ×*T*, and Gibbs free energy). Lines: calculated by the present EOS model at $T = 298$ K and $P = 6.434$ MPa.

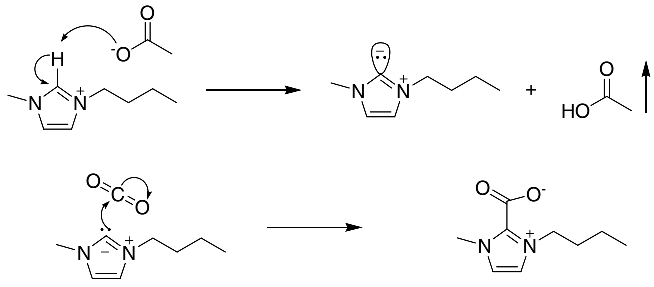

FIGURE 6. Proposed chemical reaction by Maginn [1].

when comparing the [bmim][Ac] spectrum *versus* the [bmim][Ac] with dissolved CO_2 spectrum, but it did not. Second, the TGA-IR could not detect the presence of acetic acid within detection limits.

On the other hand, the strong complex formation between CO_2 and [bmim][Ac] (or possibly with water) is clearly demonstrated by the CO_2 bubbling experiment (section 2.4) and the FT-IR and ATR-IR spectra (sections 2.7 and 2.8), as well as the thermodynamic excess functions in figure 5. In addition, the TGA-IR and microbalance solubility (absorption and desorption) experiments show that the complex formation is reversible. This reversibility without much degradation of [bmim][Ac] due to minor chemical reactions will be an important factor for the CO_2 sequestration application with [bmim][Ac] (and possibly + water).

5. Conclusions

High solubility of CO_2 in [bmim][Ac] is known in the literature [1,2]. However, the reported solubility data points are quite limited. We have re-examined the phase behavior of this binary system in more detail, and found that the phase behavior belongs to an extremely rare case; the CO_2 solubility is highly asymmetric with respect to CO_2 concentration (either extremely soluble or immiscible). Strong intermolecular attractive interactions exist, and the molecular complex formation is evident, perhaps even with a minor chemical reaction. The molecular complex has been shown to be reversible.

Acknowledgements

The authors thank Mr. Brian L. Wells, Mr. Joe Nestlerode, Mr. Steven F. Krakowski, and Mr. Glenn A. Miller at the DuPont Experimental Station for their assistance with the gas solubility measurements, VLLE measurements, NMR analysis, and TGA-IR analysis, respectively. They also thank Professor Edward J. Maginn from the University of Notre Dame for the proposed chemical reaction in figure 6. The present work was supported by DuPont Central Research and Development.

References

[1] E.J. Maginn. Design and evaluation of ionic liquids as novel CO_2 absorbents, Quarterly Technical Report to DOE. December 31, 2004; January 31, 2005; May 31, 2005; August 16, 2005; November 20, 2005; January 12, 2006.

[2] D. Chinn, D.Q. Vu, M.S. Driver, L.C. Boudreau. CO_2 removal from gas using ionic liquid absorbents, US Patent US20,060,251,558A1 (2006), November 9; US20,050,129,598A1 (2005), June 16.

[3] M.B. Shiflett, A. Yokozeki, Ind. Eng. Chem. Res. 44 (12) (2005) 4453–4464.

[4] M.B. Shiflett, A. Yokozeki, J. Chem. Eng. Data 51 (5) (2006) 1931–1939.

[5] M.B. Shiflett, A. Yokozeki, J. Phys. Chem. B 110 (29) (2006) 14436–14443.

[6] M.B. Shiflett, A. Yokozeki, J. Phys. Chem. B 111 (8) (2006) 2070–2074.

[7] E.W. Lemmon, M.O. McLinden, M.L. Huber, Standard reference data program REFPROP, version 7.0, National Institute of Standards and Technology, Gaithersburg, MD, 2002.

[8] BASF website http://www2.basf.de/en/intermed/nbd/products/ionic_liquids/.

[9] A. Yokozeki, D.J. Kasprzak, M.B. Shiflett, Phys. Chem. Chem. Phys. (2007) (submitted for publication).

[10] C.J. Pouchert, The Aldrich Library of FT-IR Spectra, Vapor Phase, first ed., vol. 3, Aldrich Chemical Company, Milwaukee, 1989, p. 759.

[11] N.B. Colthup, L.H. Daly, S.E. Wiberley, Introduction to Infrared and Raman Spectroscopy, third ed., Academic Press, New York, 1990.

[12] A. Yokozeki, M.B. Shiflett, AIChE J. 52 (11) (2006) 3952–3957.

[13] A. Yokozeki, Int. J. Thermophys. 22 (4) (2001) 1057–1071.

[14] A. Yokozeki, M.B. Shiflett, Appl. Energy (2007) (in press).

[15] J.S. Rowlinson, F.L. Swinton, Liquids and Liquid Mixtures, Butterworth, London, 1982.

[16] J.T.F. Kao, J Chem. Eng. Data 15 (1970) 362–367.

[17] A. Vetere, Chem. Eng. J. 49 (1992) 27–33.

JCT 07-47